Extended Abstracts of the 22nd (1990 International) Conference on Solid State Devices and Materials, Sendai, 1990, pp. 259-262

Analytical Model for Circuit Simulation with Quarter Micron MOSFETs: Subthreshold Characteristics

M. Miura-Mattausch and H. Jacobs

Siemens AG, Corporate Research and Development

Otto-Hahn-Ring 6, Munich 83, FRG

For deep submicron MOSFETs short-channel effects dominate the transistor characteristics. This is due to the increase of the lateral electric field. This paper provides a new simple model which includes the gradient of the lateral electric field in an analytical way. The model describes the subthreshold characteristics relating to short-channel effects correctly down to $0.1\mu m$ effective channel length L_{eff} with physical parameters $(N_{sub}, C_{ox}, V_{fb}, \phi_f)$ taken from the long-channel device.

1. Introduction

For transistors with reduced channel lengths, the drain current I_D in the subthreshold region is no more independent of the drain voltage V_D but increases in absolute value. As a result, three important phenomena are observed.[1] One is a reduction of the threshold voltage V_{th}. Second is a reduction of the body effect. Third is an increase of the subthreshold swing for increased V_D. Because of their many dimensional features, small geometry effects of MOSFETs have been investigated by two or even three dimensional numerical simulators.[2,3] However, for circuit simulations a simplified analytical model is required. Unfortunately, the widely used charge-sharing model[4] is no longer appropriate for deep submicron MOSFETs.

By reducing the channel length but keeping applied voltages and other parameters as they are, only one physical quantity is changed, that is, the lateral electric field which becomes larger. The contribution of the lateral electric field causes the 2D current flow in the channel. Several authors have shown analytical solutions of the 2D Poisson equation.[5,6] However, either the solutions are too complicated for CAD applications or rather crude approximations are made. We show here that a simple analytical model can be given by combining experiment and theory basing on physical concepts.

2. Theory

A theory can be developed by applying the Gauss law to a narrow polygon in the depletion region under the gate. Under the assumption that the lateral electric field is independent of the vertical position, we get a simple relation between the vertical electric field at the surface E_x and the gradient of the lateral electric field E_y

$$E_x(y)+\sqrt{B(\phi_s(y)-V_{sub})}E_{yy}(y) = qN_{sub}\sqrt{B\phi_s(y)}+Q, \qquad (1)$$

$$B = 2\epsilon_{Si}/(qN_{sub}), \qquad E_{yy}(y) = dE_y(y)/dy$$

where N_{sub} is the substrate doping, ϕ_s is the surface potential, and Q is the mobile charge density. At subthreshold Q can be neglected. Figure 1 shows the vertical field E_x at the surface calculated by the 2D simulator MINIMOS[2] and by Eq. 1. In the analytical calculation the lateral field gradient is taken from the MINIMOS result. The reduction of the maximum E_x observed in the MINIMOS result can be reproduced by including the lateral electric field. The reduction is known as the drain-induced barrier lowering,[7] which corresponds to the reduction of V_{th} for short-channel devices.

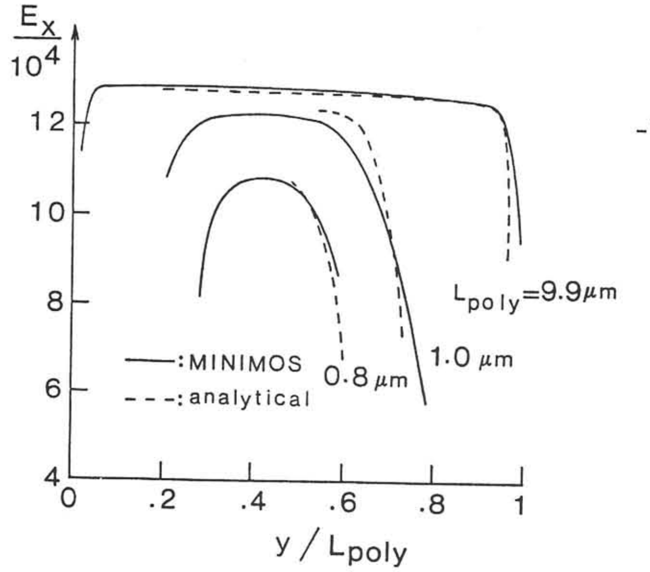

Fig.1. E_x distribution along the channel calculated by MINIMOS. Broken curves are results obtained by our theory. Applied voltages are the respective $V_G = V_{th}$ for each L_{poly}, $V_D = 4V$, and $V_{sub} = 0$.

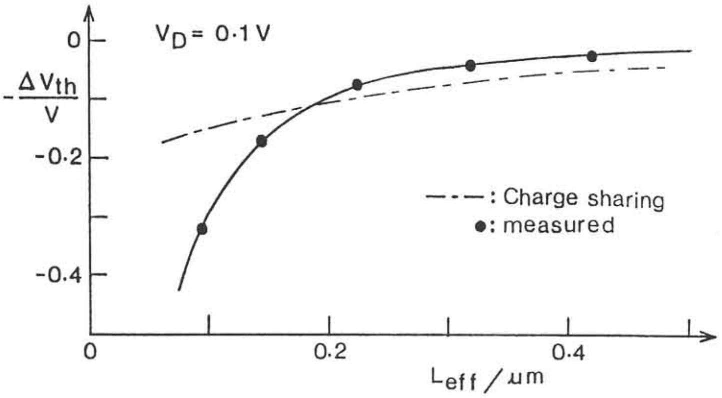

Fig.2. Calculated ΔV_{th} at $V_{sub} = 0$. The result by the charge-sharing model is shown by a dotted broken curve.

3. Results and discussion

3.1 The dependence of ΔV_{th} on L_{eff}

The threshold voltage shift from the long-channel device ΔV_{th} is represented

$$\Delta V_{th} = A\sqrt{B\phi_s E_{yy}}, \qquad (2)$$

$$A = \epsilon_{Si}/C_{ox}, \quad \phi_s = \phi_{s0} - V_{sub}$$

where ϕ_{s0} is the surface potential at threshold for a long-channel transistor. The equation can be further simplified by giving an approximation that the surface potential is a linear function of V_G at threshold, resulting in

$$\Delta V_{th} \simeq \sqrt{c}A\sqrt{B}E_{yy} \quad \text{for} \quad E_{yy} \leq 10^9\frac{V}{cm^2}, \qquad (3)$$

$$\Delta V_{th} \simeq aA^2BE_{yy}^2 \quad \text{for} \quad E_{yy} \gg 10^{10}\frac{V}{cm^2}. \qquad (4)$$

The parameters a and c define the gradient and the intersection of ϕ_{s0} as a function of V_G around threshold, which can be given by solving the Poisson equation incorporating the contribution of E_y (cf. Eq. 1). Values for $N_{sub} = 6 \times 10^{16} cm^{-3}$ are about 0.3 and 0.55V, respectively.

For an analytical model description of ΔV_{th} we need an analytical expression for the lateral field gradient. We assume a quadratic function for the lateral potential distribution. Since the potential change is not drastic in the inversion channel, this approximation should be reasonable. Figure 2 shows calculated ΔV_{th} values as a function of L_{eff} using this assumption. In the calculation no fitting parameter is used. The measured V_{th} for the long-channel transistor is used to determine the value of N_{sub}. The result of the charge-sharing model is depicted as well.

By comparing the calculated and measured ΔV_{th} values at $V_D \simeq 0$, we can estimate L_{eff}. Figure 3 shows the result. For transistors studied here L_{eff} is aboutequal to $L_{poly} - 0.5\mu m$. This is in good agreement with simulated 2D doping profiles. The L_{poly} length shorter than $0.6\mu m$ shows a saturation behavior due to the vicinity of two depletion regions from the source and the drain. For comparison measured ΔV_{th} values are also plotted in Fig.2.

The MINIMOS result shows that the magnitude of E_{yy} for short-channel devices is around $1 \times 10^9 Vcm^{-2}$. In this case Eq. 3 is a good approximation. Since the potential distribution is assumed to be a quadratic function, the dependence of ΔV_{th} is L_{eff}^{-2}. If E_{yy} becomes larger than $10^{10} Vcm^{-2}$, the dependence becomes L_{eff}^{-4}.

3.2 The dependence of ΔV_{th} on V_{sub}

Figure 4 shows the V_{th} dependence on $\sqrt{\phi_{s0} - V_{sub}}$ for different channel lengths. The agreement with measurements is very good. Thus the re-

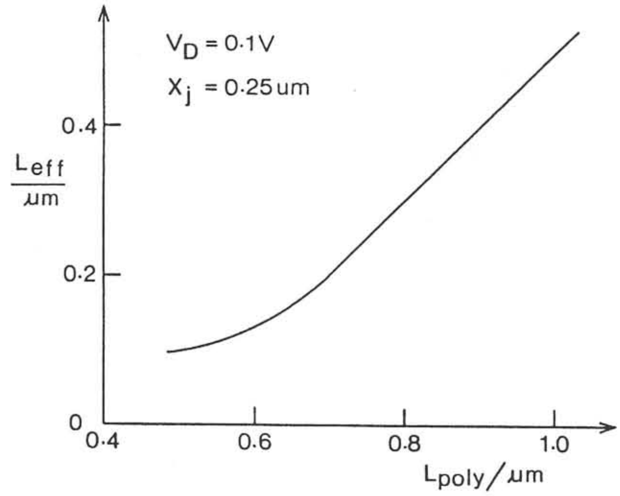

Fig.3. Calculated L_{eff} as a function of L_{poly}.

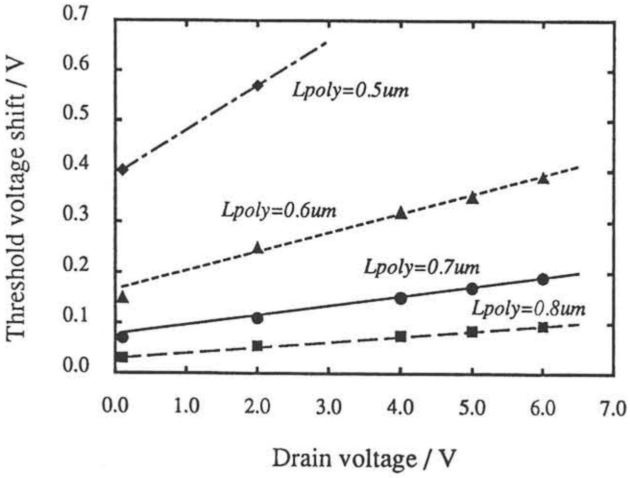

Fig.5. Measured ΔV_{th} as a function of V_D at $V_{sub} = 0$.

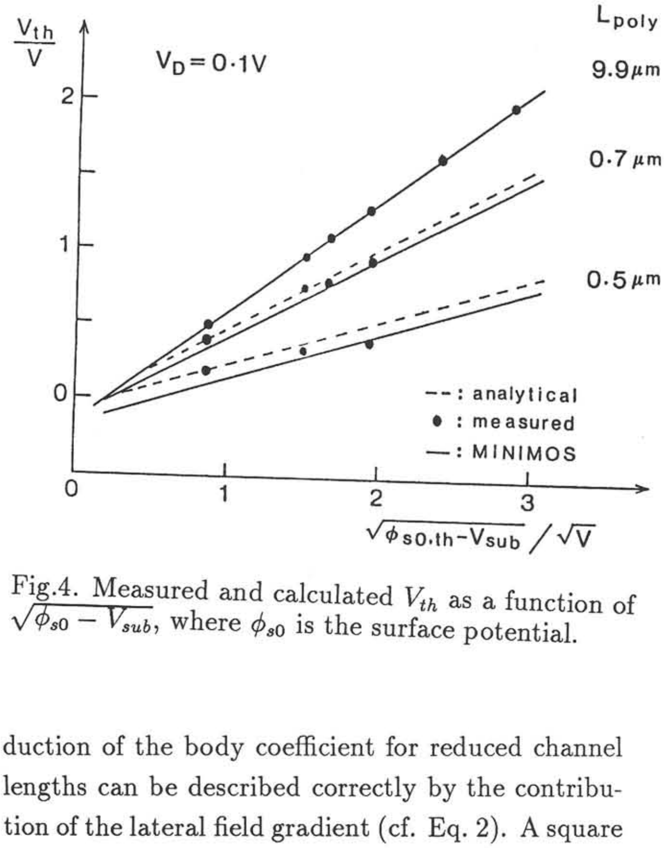

Fig.4. Measured and calculated V_{th} as a function of $\sqrt{\phi_{s0} - V_{sub}}$, where ϕ_{s0} is the surface potential.

duction of the body coefficient for reduced channel lengths can be described correctly by the contribution of the lateral field gradient (cf. Eq. 2). A square root dependence on V_{sub} can be seen as well as in the MINIMOS result. This suggests that the lateral field gradient is independent of V_{sub}. On the other hand, the charge-sharing model shows a linear dependence of ΔV_{th} on V_{sub}, which does not fit to the measurements.

3.3 The dependence of the subthreshold swing on V_D

The theory can be extended further to get an equation to evaluate the gate voltage swing S, which is given by

$$S/\log 10 = \left(1+\frac{\gamma}{2\sqrt{\phi_s}}-\frac{A\sqrt{B}}{2\sqrt{\phi_s}}E_{yy}-A\sqrt{B\phi_s}\frac{dE_{yy}}{d\phi_{s0}}\right)/\beta, \quad (5)$$

where γ is the body coefficient and β is the inverse of the thermal voltage.

As V_D increases, pinch-off occurs at the drain side. This is commonly treated as a reduction of L_{eff} by ΔL. Since the potential difference within the inversion channel is small and can be assumed to be constant in the subthreshold region, the reduction of the channel length alone causes the increase of the lateral field gradient for increased V_D. This increase causes the increase of ΔV_{th}. Thus, we can estimate ΔL by fitting calculated ΔV_{th} by Eq. 2 to measurements. Figure 5 shows the measured dependence of ΔV_{th} on V_D for different channel lengths. Linear dependence with different gradients can be seen. This linear dependence of ΔV_{th} on V_D can be written

$$\Delta V_{th}(V_D) = \Delta V_{th}(V_D \simeq 0) + gV_D. \quad (6)$$

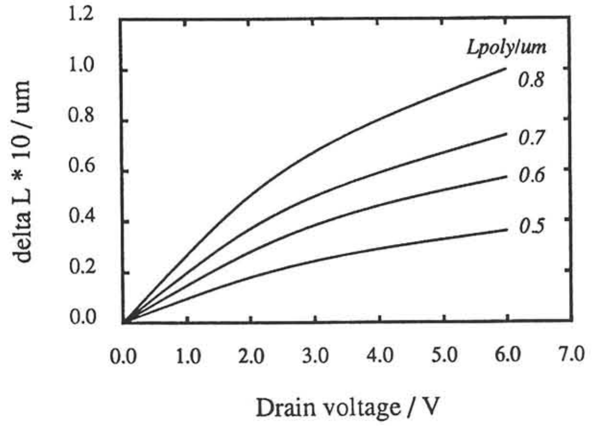

Fig.6. Calculated shortening of the channel length, ΔL.

The estimated value of g is again a linear function of $\Delta V_{th}(V_D \simeq 0)$. Because of this linearity the measured dependence of V_{th} on V_D for only one channel length is needed to get $\Delta V_{th}(V_D)$ for all channel lengths. Figure 6 shows the calculated ΔL values.

With increasing V_D values the subthreshold swing increases for short-channel transistors. This can be calculated with the ΔL derived above. The result in Fig. 7 shows good agreement with measurement.

4. Conclusion

Our model which includes the lateral electric field analytically can describe all subthreshold phenomena in a self-consistent way with physical parameters taken from the long-channel device. The potential distribution along the channel is approximated by a quadratic function, which seems suitable to reproduce measurements. Calculated reduction of the body coefficient and calculated increase of the gate voltage swing agree well with measurements with L_{eff} and its reduction as a function of V_D evaluated by combining the theory and the experiment.

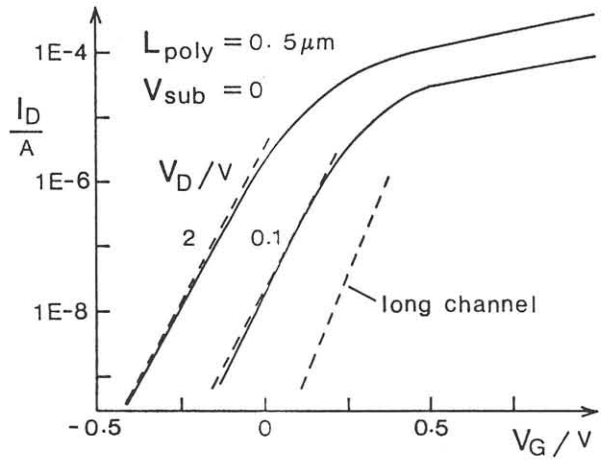

Fig.7. Subthreshold characteristics for the short-channel device. Solid curves are measurements and broken lines are calculated gradients. The gradient of the long-channel device is shown for comparison.

Acknowledgements: We would like to thank W. Neumüller for the measurements.

References

1) H. C. DeGraaff and F. M. Klaassen; *Compact Transistor Modelling for Circuit Design,* Springer-Verlag, Wien(1989).
2) S. Selberherr, A. Schuetz, and H. W. Poetzl; IEEE Trans. Electron Devices ED 27(1980) 1540.
3) R. Kasai, K. Yokoyama, A. Yoshii, and T.Sudo; IEEE Trans. Electron Devices ED 29(1982) 870.
4) L. D. Yau; Solid-State Electron. 16(1974) 1407.
5) T. Toyabe and S. Asai; IEEE TRans. Electron Devices ED 26(1979) 453.
6) K. N. Ratnakumar and J. D. Meindl; IEEE J. Solid-State Circuits SC 17 (1982) 937.
7) R. R. Troutman; IEEE Trans. Electron Devices ED 26(1979) 461.